

New Hot Subdwarf Variables from *Gaia* eDR3

Isaac D. LOPEZ^{1,2,*}, Alekzander KOSAKOWSKI³, Brad N. BARLOW² and Thomas KUPFER³

¹ Department of Physics and Astronomy, Iowa State University, Ames, IA 50011, USA

² Department of Physics, High Point University, High Point, NC 27268, USA

³ Department of Physics and Astronomy, Texas Tech University, Lubbock, TX 79409, USA

* Corresponding author: idlopez@iastate.edu

This work is distributed under the Creative Commons CC-BY 4.0 Licence.

*Paper presented at the 10th Meeting on “Hot Subdwarfs and Related Objects”
University of Liège (Belgium), June 13–17, 2022*

Abstract

We present a search for new variable hot subdwarfs from *Gaia* eDR3 using the Zwicky Transient Facility DR9 and the 2.1 m Otto Struve Telescope at McDonald Observatory. We report the discovery of 22 HW Vir binaries, 24 reflection effect binaries, and 14 ellipsoidally modulated systems. Candidate selection for our high-speed observations was based on object location on the *Gaia* color-magnitude diagram and on intrinsic variability, which we estimate from the *Gaia* G flux uncertainties. Notable discoveries include a candidate 72 min period sdB+WD binary and two short period HW Vir binaries with periods around 67 min and 79 min, which includes the shortest-period eclipsing sdB+dM/BD discovered to date.

1. Introduction

Subluminous B (sdB) type stars sit below the main-sequence and at the blue end of the horizontal branch on the Hertzsprung-Russell (HR) diagram (Heber, 2016). Most are considered to be helium-fusing objects with masses $\sim 0.5 M_{\odot}$ and thin ($< 0.02 M_{\odot}$) hydrogen layers (Heber, 1986; Saffer et al., 1994). They can form from giant stars that have had their outer layers stripped away, which can occur via binary interaction with a companion where material is lost either during a common envelope event (Paczynski, 1976; Iben and Livio, 1993) or via Roche-lobe overflow. For giant stars with main-sequence (MS) companions that undergo a common envelope, the resulting sdB+MS binaries are predicted to have periods between 0.05 and 40 days (Han et al., 2003). Systems with white dwarf (WD) companions may undergo a total of two common envelope events, leading to sdB+WD binaries with considerably shorter periods (see Heber, 2016, for a more complete discussion on the formation of sdB stars via close-binary evolution).

Hot subdwarfs with cool companions and small separations can exhibit a strong reflection effect, which comes from changes in our point of view of the tidally-locked and heated companion as it moves through its orbit (e.g., Schaffenroth et al., 2022). Systems with sufficiently high inclinations will also exhibit primary and secondary eclipses and are known as HW Vir binaries, after the prototype HW Virginis (Menzies and Marang, 1986). When combined with

spectroscopy, the eclipses allow for the masses, radii, and separation of the two stars to be determined, allowing one to distinguish between stellar and sub-stellar companions. Approximately 270 eclipsing sdB+dM/BD systems with orbital periods between 74 minutes and 19.2 hours (median 4.6 hr) have been published to date, mainly due to the efforts of the Eclipsing Reflection Effect Binaries from Optical Surveys (EREPOS) project (Schaffenroth et al., 2019), which has relied mostly on photometry from the Optical Gravitational Lensing Experiment (OGLE; Pietrukowicz et al., 2013; Soszyński et al., 2016) and the Asteroid Terrestrial-impact Last Alert System (ATLAS; Tonry et al., 2018) projects.

In this paper, we present a search of *Gaia* eDR3 for new variable hot subdwarfs using the Zwicky Transient Facility and the 2.1 m Otto Struve Telescope at McDonald Observatory. We describe our ZTF search parameters and the Otto Struve observations in Section 2. Our findings are presented in Section 3. Finally, a discussion is given in Section 4.

2. Observations

Our targets were selected from the Culpan et al. (2022) *Gaia* eDR3 catalog of 61,585 candidate hot subdwarfs. We focused on the 32,188 objects that did not appear in the Geier et al. (2019) hot subdwarf catalog from *Gaia* DR2, as the DR2 objects are the subject of another study that is in progress. Of those 32,188 objects, 19,705 have a declination > -30 deg, which is the range accessible from both Palomar and McDonald Observatory. We first checked for photometric variability using the Zwicky Transient Facility (ZTF; Bellm et al., 2019; Masci et al., 2019), before following up select targets with the 2.1 m Otto Struve Telescope at McDonald Observatory.

2.1. Zwicky Transient Facility

The Zwicky Transient Facility is a Northern sky optical survey located at Palomar Observatory in Southern California. The 47 deg^2 field-of-view allows for the entire night sky to be imaged every 1-2 days in up to three different bandpasses (g-, r-, and i-).

Our analysis is based on ZTF Data Release 9. We first searched ZTF for any available data on the 19,705 targets described in the previous section. We used the python package ZTFQUERY to download available data, using a $5''$ search radius around the *Gaia* eDR3 coordinate. Targets with ZTF coordinates separated by over $2.5''$ were treated and analyzed as individual objects. Of the 19,705 potential targets, 17,066 had at least one ZTF coordinate with at least 40 reliable observations in total among the three ZTF bands. Reliability of the data was determined with the ZTF parameter 'catflags', which is set to zero when the data has been deemed useful. To search for periodic signals in the data, we employed the VanderPlas and Ivezić (2015) multiband periodogram, which is derived from the usual Lomb-Scargle periodogram and is able to handle observations from multiple bands simultaneously.

We searched for periodic signals within the frequency range $0\text{-}72 \text{ day}^{-1}$. Data were folded on the period with the largest amplitude and twice that period, which is often necessary for eclipsing and ellipsoidally modulated systems, taking care to inspect candidate periods that

may have had amplitudes smaller than one or more alias signal. ZTF data will often have alias signals resulting from night-to-night and seasonal gaps in the observations. These signals are often found at integer day⁻¹ values, half integer values, and/or split symmetrically around the integer and half integer values below ~ 5 day⁻¹. Assigning a variability type was then based on light curve and periodogram morphologies, as well as object position on the *Gaia* color-magnitude diagram.

Orbital periods and uncertainties were obtained by fitting the corresponding signals in the periodograms with a Gaussian profile. For systems such as eclipsing and ellipsoidally modulated systems, the frequency with the largest amplitude in the periodogram usually corresponds to the first harmonic of the orbital period. For these systems, the orbital period is twice the period obtained by fitting the frequency with the largest amplitude.

2.2. 2.1 m Otto Struve Telescope

For select targets among the 2,639 that did not have sufficient ZTF data (defined as having at least 40 reliable observations among the three ZTF bands), we obtained high-speed photometry with the 2.1 m Otto Struve Telescope (OST) at McDonald Observatory, located near Fort Davis, TX. Observations were obtained with the frame-transfer ProEM instrument and a broadband BG40 filter. Calibration frames were obtained prior to the start of each night. Data were reduced using standard IRAF packages and procedures (Tody, 1986). Differential photometry was performed by dividing the flux values of the targets by a weighted-average flux value of multiple bright calibration stars.

Selection criteria for follow-up observations was based on a combination of location relative to the sdB clump on the *Gaia* color-magnitude diagram (centered at $M_G \approx 4.5$ and $G_{bp} - G_{rp} \approx -0.25$; Schaffenroth et al., 2022) and evidence of photometric variability, which we estimated using the *Gaia* flux uncertainties. Objects exhibiting photometric variability may have anomalous flux uncertainties at their given magnitudes (e.g., Guidry et al., 2021; Barlow et al., 2022).

In the left panel of Figure 1, we show the relation between the G-band flux uncertainties (normalized by the mean G-band flux and the number of observations) and the G-band magnitudes for the complete Culpan et al. (2022) sample. The solid red line is an exponential function, called $f_1(G)$, fit to all but the most anomalous points, which otherwise does not lead to a good fit to the points that make up the exponential trend. Those anomalous points are the objects most likely to be exhibiting photometric variability.

In the middle panel of Figure 1, we show the same normalized flux uncertainty, after subtracting the function $f_1(G)$. A second-order correction was then needed for objects fainter than about 18.5 mag. To correct for this, an exponential was fit by eye to the bottom portion of the data, then the corresponding symmetric function about zero, called $f_2(G)$, was also subtracted from the normalized flux error. We then use the functions $f_1(G)$ and $f_2(G)$ to define a variability index as:

$$Varindex = \sigma_G \frac{\sqrt{n_{obs}}}{\langle G \rangle} - \left(0.1236 \times 10^{-8} e^{0.77734G} + 0.0002 e^{(G-16.0)} + 0.01062 \right) \quad (1)$$

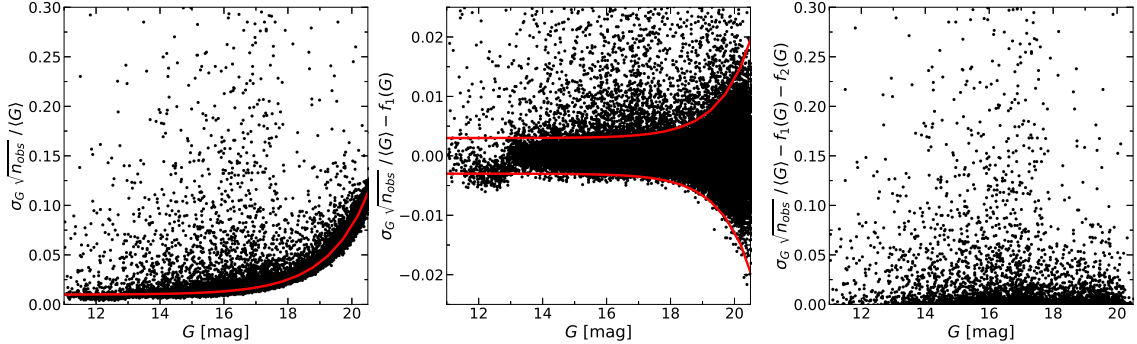


Figure 1: **Left panel:** Relation between the *Gaia* G-band flux uncertainties (normalized by the mean G-band flux and the number of observations) and the *Gaia* G-band magnitudes for the targets in the Culpan et al. (2022) catalog of hot subdwarfs. The red line is the best-fit exponential to the main bulk of points that make up the exponential trend. Objects that lie well above this line are considered to be likely variable. **Middle Panel:** Same relation as the left panel, but the exponential fit has been subtracted off. A second-order correction is needed for targets fainter than ~ 18.5 mag. The lower red line is an exponential function fit by eye, while the upper red line is the lower function reflected about the x-axis. **Right panel:** Same relation as the first panel, but corrected using the two best-fit exponential functions. We use these corrected flux uncertainties as a variability index to aid in prioritizing our ground-based observations (see Equation 1).

where σ_G is the mean G flux uncertainty, n_{obs} is the number of G flux observations, $\langle G \rangle$ is the mean G flux, and G is the mean G magnitude. The final panel in Figure 1 shows the relation between this variability index and the G magnitudes.

3. Search Results

Our search of ZTF yielded a few hundred objects that display obvious variability. The most common type of variable that we find with ZTF are cataclysmic variables (including eclipsing systems and dwarf novae). Here we present the HW Vir type binaries, reflection binaries, and ellipsoidally modulated systems that we found both with ZTF and the Otto Struve Telescope.

3.1. HW Vir Binaries

We find 25 systems with light curves like HW Vir type binaries, 22 of which are new discoveries (two resulting from our OST observations). We present these 25 systems in Table 1, along with their *Gaia* coordinates, G magnitudes, their estimated orbital periods, and the source of their discovery (ZTF or McD). The three targets with superscripted Source IDs were previously published as HW Vir type binaries. Phase-folded ZTF light curves and two additional follow-up OST light curves can be found in the Appendix. We also find one system with ZTF photometry that suggest its original classification as HW Vir type was incorrect. Below we give a brief discussion on a few systems:

J051936.46+165938.49 (*Gaia* EDR3 3394356978092225408) is a newly discovered HW

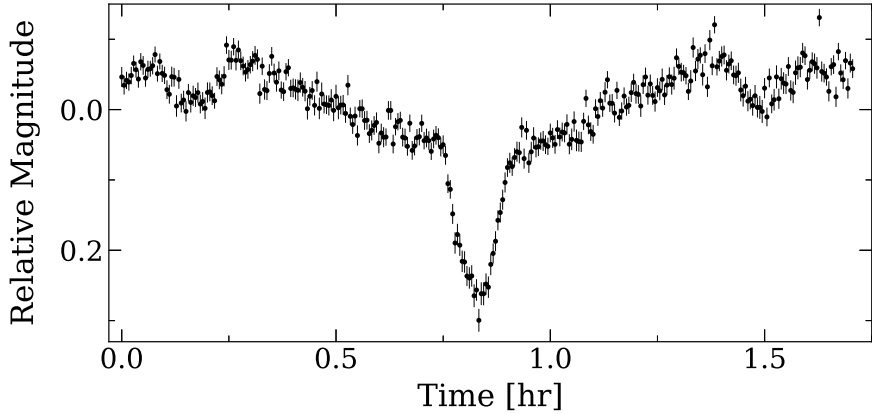


Figure 2: Discovery photometry of J0519+1659 obtained with the 2.1 m Otto Struve Telescope on 2022 January 07. This new 79 min period HW Vir is among the five shortest-period systems known to date.

Vir binary with an orbital period of roughly 79 minutes. We show the discovery high-speed photometry obtained on 2022 January 08 in Figure 2. This object has a relatively high Varindex ($V = 0.018$; see right pannel of Figure 1 and Equation 1) and is located near the hot subdwarf clump on the *Gaia* color-magnitude diagram.

ZTF J054217.01+124950.55 (*Gaia* EDR3 3340527779312131584) is a newly discovered HW Vir binary with an orbital period of 67.1712 ± 0.0018 min, making it the shortest-period HW Vir binary discovered to date. We present follow-up high-speed photometry obtained on 2022 March 05 in Figure 3. Using LAMOST spectra, Lei et al. (2019) determined this object to have an sdB primary with $T_{\text{eff}} = 31100 \pm 390$ K and $\log g = 5.59 \pm 0.05$.

J103104.50-021315.87 (*Gaia* eDR3 378171915080488755) is a new HW Vir system with a period of roughly 1.65 hr. We present the discovery high-speed photometry obtained on 2022 April 09 in Figure 4. We note that the observing conditions were particularly bad with $\sim 2.5''$ seeing, which gradually worsened to $\sim 5.5''$. Analysis of SDSS spectra by Kepler et al. (2015) give $T_{\text{eff}} = 34170$ K and $\log g = 5.73$ for the sdB star in this binary.

ZTF J194838.03+462308.57 (*Gaia* EDR3 2080272533722572288) was originally identified as an HW Vir system with a period of 0.99091 d by Schaffenroth et al. (2019). Located within $5''$ of the *Gaia* EDR3 coordinate are two ZTF objects separated by over $2.5''$ with ZTF observations spanning four years that appear to be a cataclysmic variable and a non-variable object. It is likely that the sparse OGLE data, which is what the original discovery is based on, folded in such a way to only give the appearance of a reflection effect and primary eclipse.

3.2. Reflection Binaries

We find 26 targets with light curves consistent with reflection binaries, 24 of which are reported here for the first time (one resulting from our OST observations). Similar to Table 1, we show some of their properties in Table 2. Phase-folded ZTF light curves are presented in Figure 9.

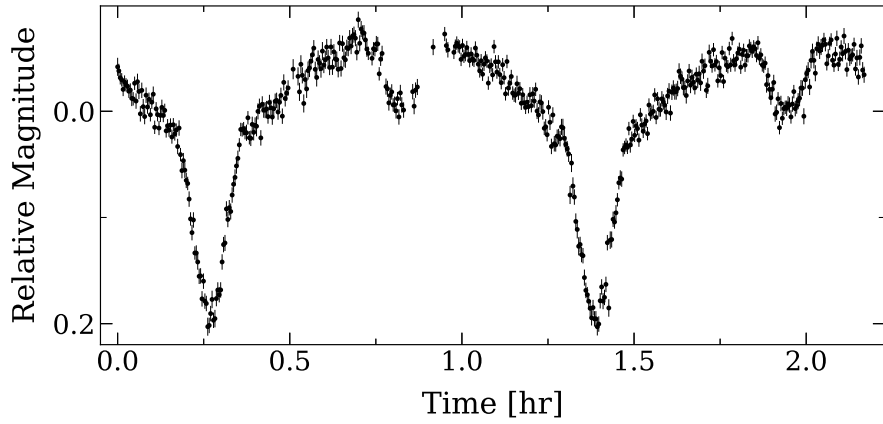


Figure 3: Follow-up high-speed photometry of ZTF J0542+1249 obtained with the 2.1 m Otto Struve Telescope on 2022 March 05. This new system has a period of 67.2 min, making it the shortest-period HW Vir system known to date.

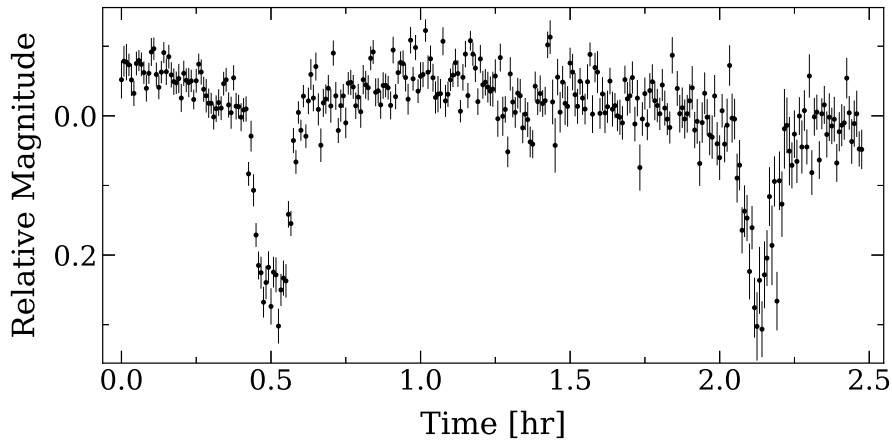


Figure 4: Discovery high-speed photometry of J1031-0213 obtained with the 2.1 m Otto Struve Telescope on 2022 April 09.

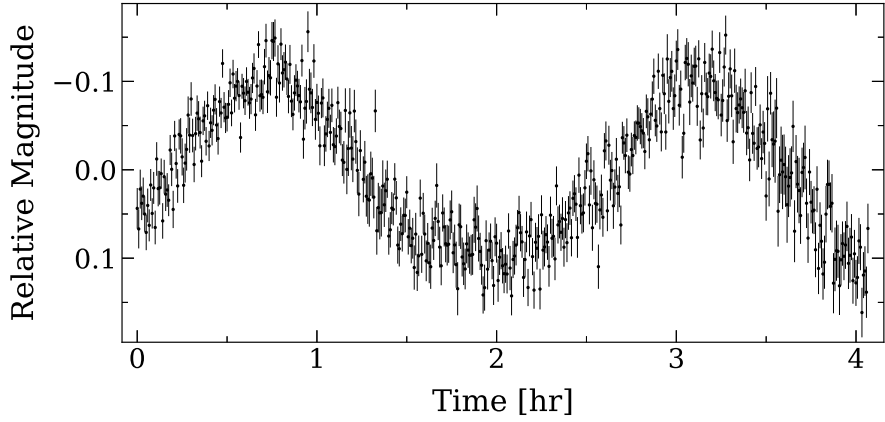


Figure 5: Discovery high-speed photometry of J0525-1143 obtained with the 2.1 m Otto Struve Telescope on 2022 February 08.

J052513.14-114345.03 (*Gaia* eDR3 3012930656340169216) is a new reflection binary with a period of roughly 2.40 hr. We show the discovery photometry obtained on 2022 February 08 in Figure 5. The broad minimum compared to the sharper maxima are typical of reflection effect binaries. However our photometry is not long enough to completely rule out the possibility of this being an ellipsoidally modulated system.

ZTF J114714.44+611531.67 (*Gaia* EDR3 859683853719128192; Feige 48) is a system containing a hot subdwarf that was first shown to exhibit pulsations in the range 340-380 s by Koen et al. (1998). A detailed spectroscopic analysis by Latour et al. (2014b) give the atmospheric parameters $T_{\text{eff}} = 29850 \pm 60$ K, $\log g = 5.46 \pm 0.01$, and $\log N(\text{He})/N(\text{H}) = -2.88 \pm 0.02$. Latour et al. (2014a) analyzed 18 spectra obtained with the 6.5 m MMT Blue Spectrograph between 2002-2013 and found a radial velocity semi-amplitude of 25.1 ± 1.4 km/s and an orbital period of 0.3436086 ± 0.0000005 d. We have found a corresponding signal in the ZTF data at a period of 0.3436042 ± 0.0000004 d, which we interpret as a reflection effect of the secondary companion.

3.3. Ellipsoidally Modulated Systems

We find a total of 15 systems with ZTF that show evidence for ellipsoidal modulation, 14 of which are reported here for the first time. Similar to Table 1, we show some of their properties in Table 3. For the orbital period, we report the period and uncertainty obtained by fitting the peak with the highest amplitude in the periodogram, which for ellipsoidally modulated systems corresponds to the first harmonic of the orbital frequency. The true orbital period is then twice the value given in Table 3. Phase-folded ZTF light cures are presented in Figure 10.

ZTF J182104.05+044150.94 (*Gaia* eDR3 4470568614447387776) is a new candidate sdB+WD binary with an orbital period of ~ 72 min. Follow up high-speed photometry obtained on 2022 April 07 is shown in Figure 6. In addition to the clear ellipsoidal modulation, the slightly off-set maxima suggest this system may be exhibiting Doppler beaming.

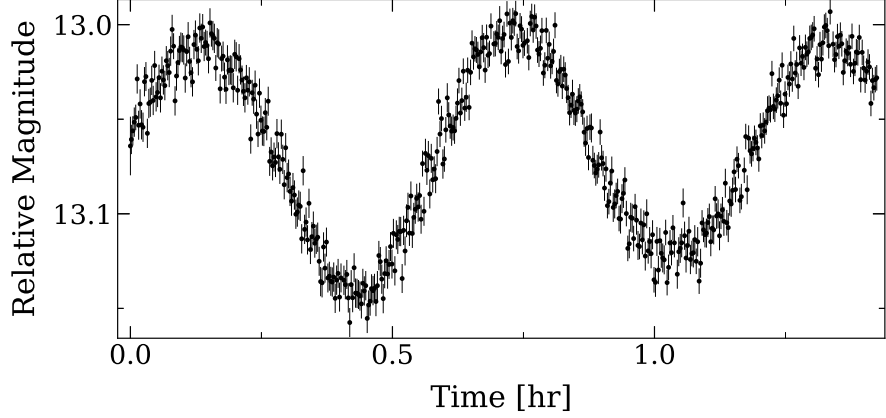


Figure 6: High-speed photometry of ZTF J1821+0441, a new candidate sdB+WD binary with a period of 72 min, obtained with the 2.1 m Otto Struve Telescope on 2022 April 07.

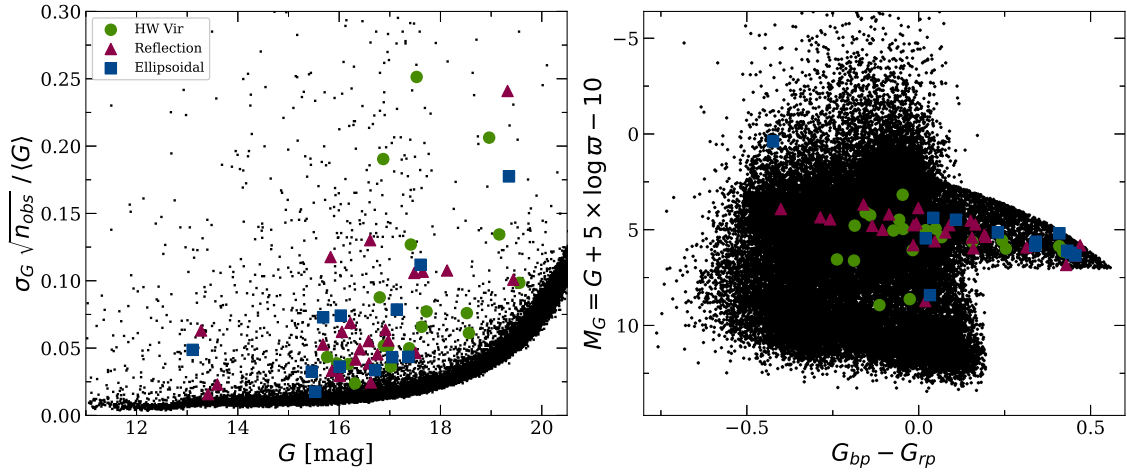


Figure 7: Left Panel: Relation between the normalized G flux uncertainty and G magnitude for objects in the Culpan et al. (2022) catalog. Superimposed are the locations of the objects presented in Section 3. **Right Panel:** The corresponding *Gaia* color-magnitude diagram for objects in the left panel.

4. Discussion

In the left panel of Figure 7, we show the relation between the (corrected and normalized) *Gaia* G flux uncertainties and the G magnitudes for the entire Culpan et al. (2022) catalog of hot subdwarfs. Superimposed are the locations of objects whose variability we discovered with ZTF. In the right panel, we show the corresponding *Gaia* color-magnitude diagram. We find that those ZTF variable objects are among the top 5% most variable objects, as ranked by Equation 1, illustrating the usefulness of the flux uncertainties for estimating stellar variability. Lastly, of the objects within the top 5%, $\sim 40\%$ of those that had sufficient ZTF data showed clear signs of photometric variability.

To search for periodic signals in the ZTF data, we computed periodograms over the frequency range $0\text{--}72 \text{ day}^{-1}$. This upper bound corresponds to period searches down to 20 minutes.

While most of the variables that we are after (reflection, HW Vir, and ellipsoidally modulated binaries) are expected to have periods longer than 20 minutes, we may have missed objects such as ultra-short period binaries and pulsators. This sacrifice was made with computational resources in mind.

ZTF J0542+1249 ($P = 67.2$ min, $G = 16.8$) and J0519+1659 ($P = 79.2$ min, $G = 18.4$) are among the five shortest-period HW Vir systems known. ZTF J0542+1249 now holds the record for the shortest period HW Vir, previously held by OGLE-BLG-ECL-000036 at 74.9 min (Schaffenroth et al., 2019). These two systems are likely the only two short-period systems bright enough to obtain phase resolved spectroscopy with existing facilities. A detailed photometric and spectroscopic analysis of these two systems is in progress and will be presented in a later publication.

HW Vir binaries have physical properties that are fairly straight-forward to solve for, especially when compared to, e.g., cataclysmic variables or X-ray binaries. Since hot subdwarfs have recently evolved from a common envelope, they are ideal systems for investigating this poorly understood phase of binary evolution. Characterizing the Galactic population would allow us to place empirical constraints on formation theory of hot subdwarfs, such as on the minimum mass needed to eject the envelope of a giant star and the minimum mass able to survive the common envelope phase.

We will soon gain access to an entirely new set of variables in the southern hemisphere with future surveys like BlackGEM (Bloemen et al., 2016) and The Vera Rubin Observatory’s Legacy Survey of Space and Time (LSST Science Collaboration et al., 2009; Ivezić et al., 2019). Continuing to build the catalog of known hot subdwarfs will allow us to eventually use tools from statistics to further understand these stars.

Acknowledgments

We would like to thank John Kuehne and Coyne Gibson for their support while observing at McDonald Observatory. I.D.L. and B.N.B. acknowledge support by NSF grant AST-1812874.

This work has made use of data from the European Space Agency (ESA) mission *Gaia* (<https://www.cosmos.esa.int/gaia>), processed by the *Gaia* Data Processing and Analysis Consortium (DPAC, <https://www.cosmos.esa.int/web/gaia/dpac/consortium>). Funding for the DPAC has been provided by national institutions, in particular the institutions participating in the *Gaia* Multilateral Agreement.

Based on observations obtained with the Samuel Oschin 48-inch Telescope at the Palomar Observatory as part of the Zwicky Transient Facility project. ZTF is supported by the National Science Foundation under Grant No. AST-2034437 and a collaboration including Caltech, IPAC, the Weizmann Institute for Science, the Oskar Klein Center at Stockholm University, the University of Maryland, Deutsches Elektronen-Synchrotron and Humboldt University, the TANGO Consortium of Taiwan, the University of Wisconsin at Milwaukee, Trinity College Dublin, Lawrence Livermore National Laboratories, and IN2P3, France. Operations are conducted by COO, IPAC, and UW.

The ztfquery code was funded by the European Research Council (ERC) under the European Union's Horizon 2020 research and innovation programme (grant agreement n°759194 - USNAC, PI: Rigault).

Further Information

Authors' ORCID identifiers

0000-0002-0009-409X (Isaac D. LOPEZ)
0000-0002-8558-4353 (Alekzander KOSAKOWSKI)
0000-0002-8558-4353 (Brad N. BARLOW)
0000-0002-6540-1484 (Thomas KUPFER)

Author contributions

IDL - Methodology, Observing, Data Analysis, Writing
AK - Observing, Data Analysis, Review/Editing
BNB - Supervision
TK - Resources

Conflicts of interest

The authors declare no conflict of interest.

Table 1: HW Vir binaries found in our search of the Culpan et al. (2022) catalog of hot sub-dwarfs. We give their Gaia eDR3 Source ID, RA, DEC, and G-band magnitude, their orbital period (found using ZTF data, when available, otherwise estimated from the McDonald data), and the source of discovery (ZTF or McD). Source IDs with a superscript have previously been published. Phase-folded ZTF light curves are presented in Figure 8.

Gaia eDR3 Source ID	RA [Gaia]	DEC [Gaia]	G [mag]	Period [hr]	Source
3340527779312131584	05 42 17.01	+12 49 50.55	16.80	1.11952(3)	ZTF
3394356978092225408	05 19 36.46	+16 59 38.49	18.36	1.32(1)	McD
1974922032534272768	21 58 15.44	+45 46 30.67	18.52	1.56839(6)	ZTF
3781719150804887552	10 31 04.50	-02 13 15.87	18.76	1.65(1)	McD
1864121982365984128	20 40 46.57	+34 07 02.74	17.41	1.79238(4)	ZTF
1965596391525733120	21 20 42.46	+40 14 34.71	17.02	1.95997(5)	ZTF
404233147851724928	01 04 40.72	+50 26 47.91	19.56	2.13495(6)	ZTF
5646693014160460416	08 27 50.10	-27 36 37.87	16.87	2.42578(9)	ZTF
4499413855323482752	17 47 09.70	+12 59 58.42	18.96	2.57096(7)	ZTF
889263087329948928	06 52 19.65	+31 19 43.09	17.73	2.62181(9)	ZTF
3356702316908290816	06 25 30.41	+14 44 07.38	15.96	2.64405(9)	ZTF
4247741145588749312	20 06 52.77	+04 16 13.22	20.08	2.99430(9)	ZTF
a 1978219536621659136	21 31 41.44	+46 54 29.98	17.38	3.11923(11)	ZTF
2025568909688842112	19 22 40.88	+26 24 15.50	17.63	3.64669(28)	ZTF
2677056689010163456	22 08 23.65	-01 15 34.29	18.56	3.75612(17)	ZTF
5619901038222784768	07 24 29.82	-21 10 22.23	17.53	3.92313(20)	ZTF
2036933560623428096	19 05 41.02	+27 03 53.17	19.16	3.93218(16)	ZTF
b 2051078953817324672	19 20 59.77	+37 22 19.98	15.76	4.05491(22)	ZTF
1968673301791825920	21 18 12.61	+40 47 27.57	16.71	4.08821(22)	ZTF
2073906430127699712	19 52 44.50	+41 44 02.27	16.88	5.2056(7)	ZTF
391755859836391680	00 29 53.98	+50 32 31.02	16.18	5.4170(4)	ZTF
1870696920156909440	20 49 15.39	+36 04 38.81	18.29	5.9380(4)	ZTF
1869815700251723392	20 58 03.60	+36 04 59.16	16.34	6.0059(4)	ZTF
4290201742045065344	19 40 06.11	+04 21 34.75	16.31	7.4108(6)	ZTF
c 1819387836386252672	20 36 27.73	+23 50 22.55	16.97	8.6334(9)	ZTF

a. Keller et al. (2022); b. Schaffenroth et al. (2014); c. Schaffenroth et al. (2019)

Table 2: Similar to Table 1, except for the reflection effect binaries found in our search of the Culpan et al. (2022) catalog of hot subdwarfs. Source IDs with a superscript have previously been published. Phase-folded ZTF light curves are presented in Figure 9.

Gaia eDR3 Source ID	RA [Gaia]	DEC [Gaia]	G [mag]	Period [hr]	Source
141419254284409472	02 49 04.88	+36 43 50.27	15.68	1.252210(23)	ZTF
3012930656340169216	05 25 13.14	-11 43 45.03	18.60	2.40(1)	McD
397243689870740096	01 26 31.49	+44 58 34.30	19.44	2.55980(10)	ZTF
2652639593773429120	22 40 40.77	-02 07 32.66	17.14	2.63589(8)	ZTF
1988952419378436736	22 57 48.41	+50 32 00.52	16.91	2.77613(12)	ZTF
5712660963048315776	07 49 30.05	-20 25 13.87	17.48	2.81315(11)	ZTF
1909051218625565824	22 29 18.12	+39 38 05.71	19.32	3.00906(13)	ZTF
2073383504960326400	19 53 57.10	+39 15 37.58	17.51	3.49288(15)	ZTF
3051336979759781888	07 10 19.46	-08 45 45.38	16.97	4.30544(23)	ZTF
1914301803258669440	23 05 36.41	+34 41 54.20	13.27	4.77051(29)	ZTF
1961481091294773888	22 11 13.61	+43 00 52.65	18.13	5.0575(4)	ZTF
1995735963743550336	23 17 07.69	+53 28 32.79	16.76	5.2489(4)	ZTF
2003045070375592576	22 38 20.11	+53 51 56.21	16.61	5.3074(5)	ZTF
4510124820868871424	18 33 20.15	+15 46 59.48	16.59	5.3411(4)	ZTF
a 1896805240366383360	22 03 51.39	+30 02 55.95	13.60	5.9199(4)	ZTF
4505290680570630656	18 45 22.98	+12 06 36.81	15.83	6.2622(4)	ZTF
4132826959121759872	16 59 35.35	-17 13 26.28	16.05	7.0249(6)	ZTF
4202377116941956096	18 54 12.93	-10 04 36.18	16.33	7.1980(5)	ZTF
4505844147236206464	18 44 50.54	+14 15 39.50	16.22	7.3813(7)	ZTF
2039845003005644928	19 21 17.62	+31 52 49.56	16.63	7.9296(7)	ZTF
4318504751925184768	19 41 50.28	+15 19 55.29	16.58	8.2312(9)	ZTF
b 859683853719128192	11 47 14.44	+61 15 31.67	13.41	8.2465(10)	ZTF
2000507294460226688	22 29 14.99	+51 26 42.90	15.86	8.6101(10)	ZTF
2003890457378405760	22 48 30.63	+56 12 02.70	16.01	9.5840(13)	ZTF
4081247494274264704	19 13 19.77	-21 54 39.74	16.41	10.0255(10)	ZTF
3376224038487974656	06 29 33.26	+21 50 07.45	17.65	10.7998(15)	ZTF

a. Schaffenroth et al. (2022); b. Schaffenroth et al. (2019)

Table 3: Similar to Table 1, except for the ellipsoidally modulated binaries found in our search of the Culpan et al. (2022) catalog of hot subdwarfs. Source ID with a superscript has previously been published. For the orbital period, we report the period found by fitting the fundamental mode in the periodogram, which corresponds to 1/2 the true value. Phase-folded ZTF light curves are presented in Figure 10.

Gaia eDR3 Source ID	RA [Gaia]	DEC [Gaia]	G [mag]	Period / 2 [hr]	Source
^a 2163801981105229184	20 55 15.98	+46 51 06.38	17.61	0.4695650(25)	ZTF
4470568614447387776	18 21 04.05	+04 41 50.94	16.01	0.601165(4)	ZTF
3112602038233556736	07 03 45.20	+00 32 10.71	16.71	0.841652(8)	ZTF
3053571840222008192	07 29 09.36	-08 35 31.52	15.68	1.94946(5)	ZTF
4358250649810243584	16 35 15.83	-01 53 51.03	15.88	2.02781(5)	ZTF
1315840437462118400	16 14 57.49	+27 20 30.62	17.80	2.23252(6)	ZTF
2708889818377067264	22 19 33.87	+06 49 22.86	17.37	2.30002(6)	ZTF
437710871734050432	02 51 19.02	+47 53 58.68	19.35	2.37023(7)	ZTF
2652639593773429120	22 40 40.77	-02 07 32.66	17.14	2.63589(8)	ZTF
6848618205821392768	20 30 48.67	-24 33 04.26	16.03	3.05179(9)	ZTF
4512536977593172864	18 43 36.22	+18 35 41.03	15.53	3.50717(13)	ZTF
2845910240171925632	23 18 07.31	+28 34 58.45	15.46	3.62690(17)	ZTF
878465711345150336	07 44 49.44	+29 07 09.27	16.17	3.99787(21)	ZTF
1968809331997065088	21 19 28.92	+41 39 50.37	17.05	5.6072(4)	ZTF
4030308460578827264	12 14 48.52	+36 38 49.12	13.11	6.8845(6)	ZTF

a. Kupfer et al. (2020)

References

- Barlow, B. N., Corcoran, K. A., Parker, I. M., Kupfer, T., Németh, P., Hermes, J. J., Lopez, I. D., Frondorf, W. J., Vestal, D. and Holden, J. (2022) New variable hot subdwarf stars identified from anomalous gaia flux errors, observed by TESS, and classified via Fourier diagnostics. *Astrophys. J.*, 928(1), 20. <https://doi.org/10.3847/1538-4357/ac49f1>.
- Bellm, E. C., Kulkarni, S. R., Graham, M. J., Dekany, R., Smith, R. M., Riddle, R., Masci, F. J., Helou, G., Prince, T. A., Adams, S. M., Barbarino, C., Barlow, T., Bauer, J., Beck, R., Belicki, J., Biswas, R., Blagorodnova, N., Bodewits, D., Bolin, B., Brinnel, V., Brooke, T., Bue, B., Bulla, M., Burruss, R., Cenko, S. B., Chang, C.-K., Connolly, A., Coughlin, M., Cromer, J., Cunningham, V., De, K., Delacroix, A., Desai, V., Duev, D. A., Eadie, G., Farnham, T. L., Feeney, M., Feindt, U., Flynn, D., Franckowiak, A., Frederick, S., Fremling, C., Gal-Yam, A., Gezari, S., Giomi, M., Goldstein, D. A., Golkhou, V. Z., Goobar, A., Groom, S., Hacopians, E., Hale, D., Henning, J., Ho, A. Y. Q., Hover, D., Howell, J., Hung, T., Huppenkothen, D., Imel, D., Ip, W.-H., Ivezić, Ž., Jackson, E., Jones, L., Juric, M., Kasliwal, M. M., Kaspi, S., Kaye, S., Kelley, M. S. P., Kowalski, M., Kramer, E., Kupfer, T., Landry, W., Laher, R. R., Lee, C.-D., Lin, H. W., Lin, Z.-Y., Lunnan, R., Giomi, M.,

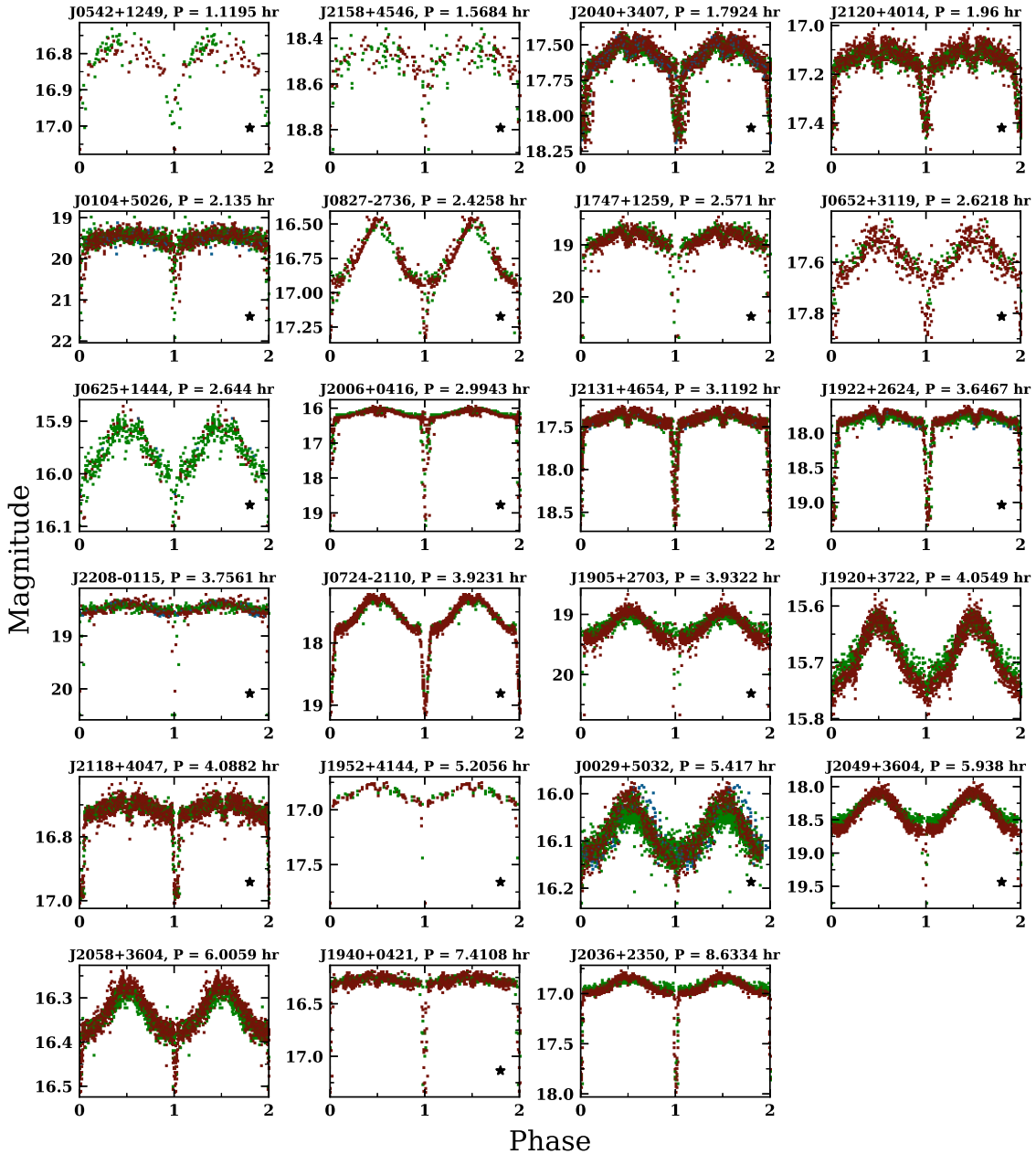


Figure 8: Phase-folded ZTF light curves of the HW Vir systems found from *Gaia* eDR3. Data were phase-folded on the orbital period and mean r- and i-band magnitudes were shifted to match the mean g-band magnitude. Two complete phases have been plotted for visual clarity. Objects with a black star are new discoveries.

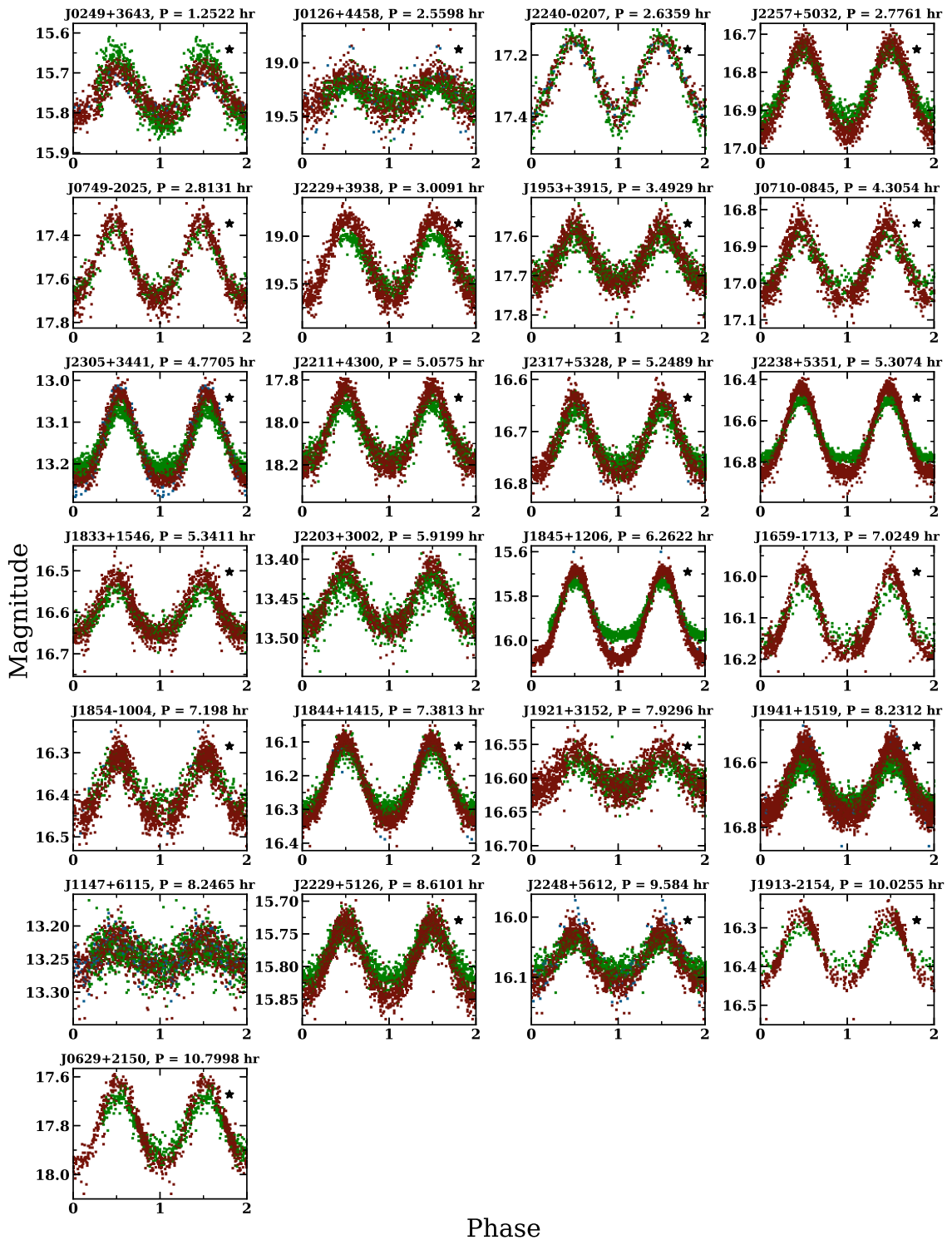


Figure 9: Phase-folded ZTF light curves of the reflection systems from *Gaia* eDR3. Data were phase-folded on the orbital period and mean r- and i-band magnitudes were shifted to match the mean g-band magnitude. Two complete phases have been plotted for visual clarity. Objects with a black star are new discoveries.

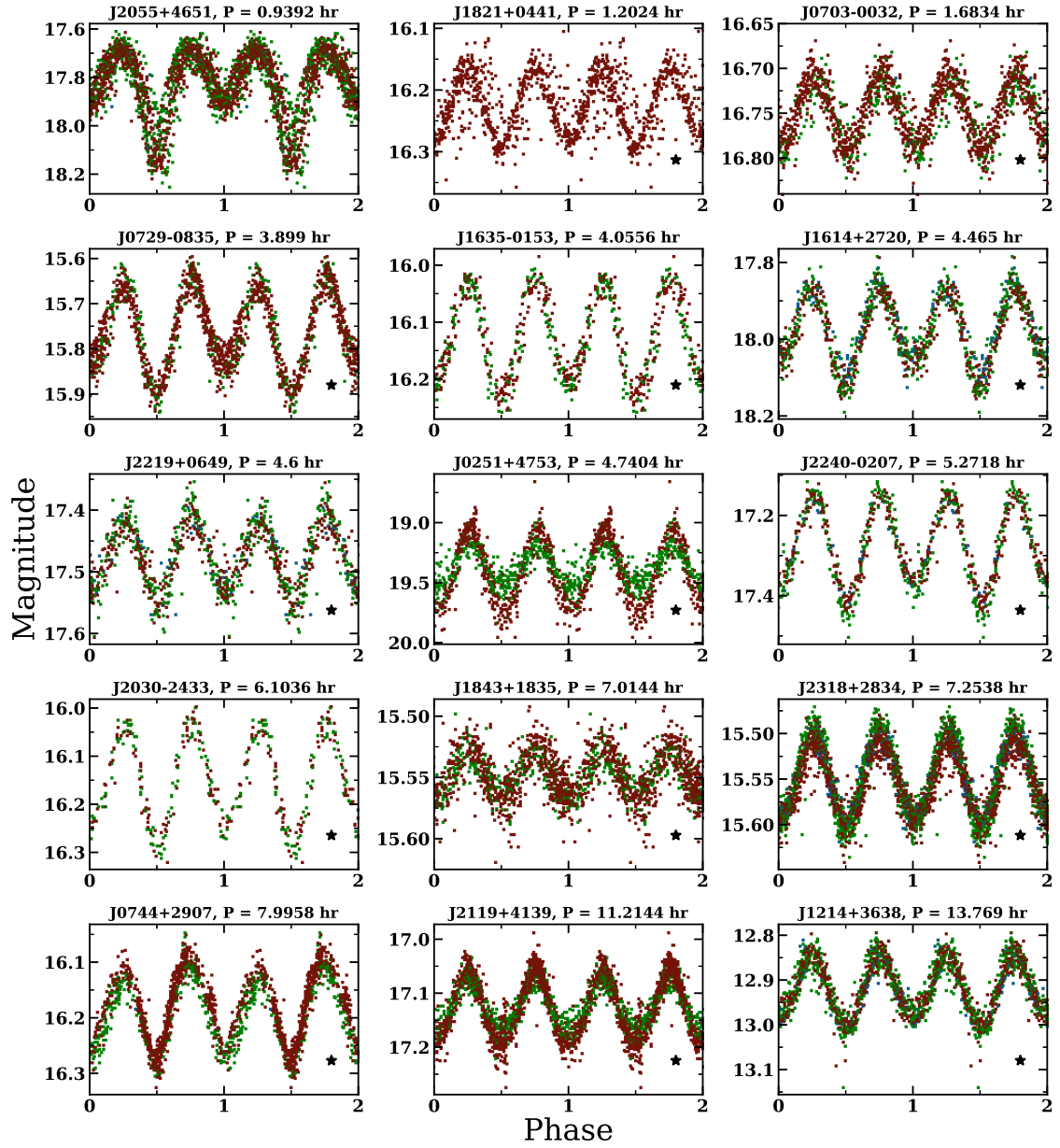


Figure 10: Phase-folded ZTF light curves of the ellipsoidally modulated systems from *Gaia* eDR3. Data were on the orbital period and mean r- and i-band magnitudes were shifted to match the mean g-band magnitude. Two complete phases have been plotted for visual clarity. Objects with a black star are new discoveries.

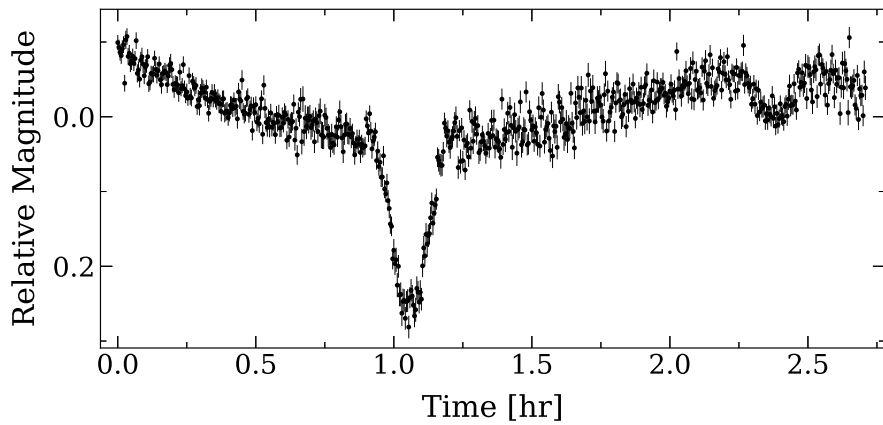


Figure 11: Follow-up high-speed photometry of J0652+3119 obtained with the 2.1 m Otto Struve Telescope on 2022 February 07. This new HW Vir system has a period of 2.62181 ± 0.00009 hr.

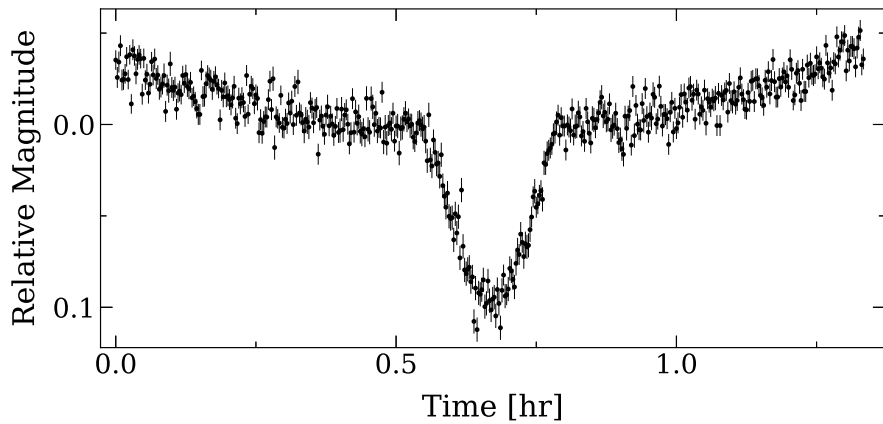


Figure 12: Follow-up high-speed photometry of ZTF J0625+1444 obtained with the 2.1 m Otto Struve Telescope on 2021 December 07. This new HW Vir system has a period of 2.64405 ± 0.00009 hr.

Mahabal, A., Mao, P., Miller, A. A., Monkewitz, S., Murphy, P., Ngeow, C.-C., Nordin, J., Nugent, P., Ofek, E., Patterson, M. T., Penprase, B., Porter, M., Rauch, L., Rebbapragada, U., Reiley, D., Rigault, M., Rodriguez, H., van Roestel, J., Rusholme, B., van Santen, J., Schulze, S., Shupe, D. L., Singer, L. P., Soumagnac, M. T., Stein, R., Surace, J., Sollerman, J., Szkody, P., Taddia, F., Terek, S., Van Sistine, A., van Velzen, S., Vestrand, W. T., Walters, R., Ward, C., Ye, Q.-Z., Yu, P.-C., Yan, L. and Zolkower, J. (2019) The Zwicky Transient Facility: System overview, performance, and first results. *Publ. Astron. Soc. Pac.*, 131(995), 018002. <https://doi.org/10.1088/1538-3873/aaecbe>.

Bloemen, S., Groot, P., Woudt, P., Klein Wolt, M., McBride, V., Nelemans, G., Körding, E., Pretorius, M. L., Roelfsema, R., Bettonvil, F., Balster, H., Bakker, R., Dolron, P., van Elteren, A., Elswijk, E., Engels, A., Fender, R., Fokker, M., de Haan, M., Hagoort, K., de Hoog, J., ter Horst, R., van der Kevie, G., Kozłowski, S., Kragt, J., Lech, G., Le Poole, R., Lesman, D., Morren, J., Navarro, R., Paalberends, W.-J., Paterson, K., Pawłaszek, R., Pessemier, W., Raskin, G., Rutten, H., Scheers, B., Schuil, M. and Sybilska, P. W. (2016) MeerLICHT and BlackGEM: custom-built telescopes to detect faint optical transients. In *Ground-based and Airborne Telescopes VI*, edited by Hall, H. J., Gilmozzi, R. and Marshall, H. K., vol. 9906 of *Society of Photo-Optical Instrumentation Engineers (SPIE) Conference Series*. <https://doi.org/10.1117/12.2232522>.

Culpan, R., Geier, S., Pelisoli, I., Reindl, N., Gentile Fusillo, N. and Vorontseva, A. (2022) The population of hot subdwarf stars studied with *Gaia* – IV. Catalogues of hot subluminous stars based on gaia EDR3. *arXiv e-prints*, arXiv:2203.07938.

Geier, S., Raddi, R., Gentile Fusillo, N. P. and Marsh, T. R. (2019) The population of hot subdwarf stars studied with *Gaia*. II. the *Gaia* DR2 catalogue of hot subluminous stars. *Astron. Astrophys.*, 621, A38. <https://doi.org/10.1051/0004-6361/201834236>.

Guidry, J. A., Vanderbosch, Z. P., Hermes, J. J., Barlow, B. N., Lopez, I. D., Boudreux, T. M., Corcoran, K. A., Bell, K. J., Montgomery, M. H., Heintz, T. M., Castanheira, B. G., Reding, J. S., Dunlap, B. H., Winget, D. E., Winget, K. I. and Kuehne, J. W. (2021) I Spy transits and pulsations: Empirical variability in white dwarfs using gaia and the Zwicky Transient Facility. *Astrophys. J.*, 912, 125. <https://doi.org/10.3847/1538-4357/abee68>.

Han, Z., Podsiadlowski, P., Maxted, P. F. L. and Marsh, T. R. (2003) The origin of subdwarf B stars – II. *Mon. Not. R. Astron. Soc.*, 341(2), 669–691. <https://doi.org/10.1046/j.1365-8711.2003.06451.x>.

Heber, U. (1986) The atmosphere of subluminous B stars. II. Analysis of 10 helium poor subdwarfs and the birthrate of sdB stars. *Astron. Astrophys.*, 155, 33–45.

Heber, U. (2016) Hot subluminous stars. *Publ. Astron. Soc. Pac.*, 128(966), 082001. <https://doi.org/10.1088/1538-3873/128/966/082001>.

Iben, I., Jr. and Livio, M. (1993) Common envelopes in binary star evolution. *Publ. Astron. Soc. Pac.*, 105, 1373. <https://doi.org/10.1086/133321>.

Ivezić, Ž., Kahn, S. M., Tyson, J. A., Abel, B., Acosta, E., Allsman, R., Alonso, D., AlSayyad, Y., Anderson, S. F., Andrew, J., Angel, J. R. P., Angeli, G. Z., Ansari, R., Antilogus, P., Araujo, C., Armstrong, R., Arndt, K. T., Astier, P., Aubourg, É., Auza, N., Axelrod, T. S., Bard, D. J., Barr, J. D., Barrau, A., Bartlett, J. G., Bauer, A. E., Bauman, B. J., Baumont, S., Bechtol, E., Bechtol, K., Becker, A. C., Becla, J., Beldica, C., Bellavia, S., Bianco, F. B., Biswas, R., Blanc, G., Blazek, J., Blandford, R. D., Bloom, J. S., Bogart, J., Bond, T. W., Booth, M. T., Borgland, A. W., Borne, K., Bosch, J. F., Boutigny, D., Brackett, C. A., Bradshaw, A., Brandt, W. N., Brown, M. E., Bullock, J. S., Burchat, P., Burke, D. L., Cagnoli, G., Calabrese, D., Callahan, S., Callen, A. L., Carlin, J. L., Carlson, E. L., Chandrasekharan, S., Charles-Emerson, G., Chesley, S., Cheu, E. C., Chiang, H.-F., Chiang, J., Chirino, C., Chow, D., Ciardi, D. R., Claver, C. F., Cohen-Tanugi, J., Cockrum, J. J., Coles, R., Connolly, A. J., Cook, K. H., Cooray, A., Covey, K. R., Cribbs, C., Cui, W., Cutri, R., Daly, P. N., Daniel, S. F., Daruich, F., Daubard, G., Daues, G., Dawson, W., Delgado, F., Dellapenna, A., de Peyster, R., de Val-Borro, M., Digel, S. W., Doherty, P., Dubois, R., Dubois-Felsmann, G. P., Durech, J., Economou, F., Eifler, T., Eracleous, M., Emmons, B. L., Fausti Neto, A., Ferguson, H., Figueroa, E., Fisher-Levine, M., Focke, W., Foss, M. D., Frank, J., Freemont, M. D., Gangler, E., Gawiser, E., Geary, J. C., Gee, P., Geha, M., Gessner, C. J. B., Gibson, R. R., Gilmore, D. K., Glanzman, T., Glick, W., Goldina, T., Goldstein, D. A., Goodenow, I., Graham, M. L., Gressler, W. J., Gris, P., Guy, L. P., Guyonnet, A., Haller, G., Harris, R., Hascall, P. A., Haupt, J., Hernandez, F., Herrmann, S., Hileman, E., Hoblitt, J., Hodgson, J. A., Hogan, C., Howard, J. D., Huang, D., Huffer, M. E., Ingraham, P., Innes, W. R., Jacoby, S. H., Jain, B., Jammes, F., Jee, M. J., Jenness, T., Jernigan, G., Jevremović, D., Johns, K., Johnson, A. S., Johnson, M. W. G., Jones, R. L., Juramy-Gilles, C., Jurić, M., Kalirai, J. S., Kallivayalil, N. J., Kalmbach, B., Kantor, J. P., Karst, P., Kasliwal, M. M., Kelly, H., Kessler, R., Kinnison, V., Kirkby, D., Knox, L., Kotov, I. V., Krabbendam, V. L., Krughoff, K. S., Kubánek, P., Kuczewski, J., Kulkarni, S., Ku, J., Kurita, N. R., Lage, C. S., Lambert, R., Lange, T., Langton, J. B., Le Guillou, L., Levine, D., Liang, M., Lim, K.-T., Lintott, C. J., Long, K. E., Lopez, M., Lotz, P. J., Lupton, R. H., Lust, N. B., MacArthur, L. A., Mahabal, A., Mandelbaum, R., Markiewicz, T. W., Marsh, D. S., Marshall, P. J., Marshall, S., May, M., McKercher, R., McQueen, M., Meyers, J., Migliore, M., Miller, M., Mills, D. J., Miraval, C., Moeyens, J., Moolekamp, F. E., Monet, D. G., Moniez, M., Monkewitz, S., Montgomery, C., Morrison, C. B., Mueller, F., Muller, G. P., Muñoz Arancibia, F., Neill, D. R., Newbry, S. P., Nief, J.-Y., Nomerotski, A., Nordby, M., O'Connor, P., Oliver, J., Olivier, S. S., Olsen, K., O'Mullane, W., Ortiz, S., Osier, S., Owen, R. E., Pain, R., Palecek, P. E., Parejko, J. K., Parsons, J. B., Pease, N. M., Peterson, J. M., Peterson, J. R., Petravick, D. L., Libby Petrick, M. E., Petry, C. E., Pierfederici, F., Pietrowicz, S., Pike, R., Pinto, P. A., Plante, R., Plate, S., Plutchak, J. P., Price, P. A., Prouza, M., Radeka, V., Rajagopal, J., Rasmussen, A. P., Regnault, N., Reil, K. A., Reiss, D. J., Reuter, M. A., Ridgway, S. T., Riot, V. J., Ritz, S., Robinson, S., Roby, W., Roodman, A., Rosing, W., Roucelle, C., Rumore, M. R., Russo, S., Saha, A., Sassolas, B., Schalk, T. L., Schellart, P., Schindler, R. H., Schmidt, S., Schneider, D. P., Schneider, M. D., Schoening, W., Schumacher, G., Schwamb, M. E., Sebag, J., Selvy, B., Sembroski, G. H., Seppala, L. G., Serio, A., Serrano, E., Shaw, R. A., Shipsey, I., Sick,

J., Silvestri, N., Slater, C. T., Smith, J. A., Smith, R. C., Sobhani, S., Soldahl, C., Storrie-Lombardi, L., Stover, E., Strauss, M. A., Street, R. A., Stubbs, C. W., Sullivan, I. S., Sweeney, D., Swinbank, J. D., Szalay, A., Takacs, P., Tether, S. A., Thaler, J. J., Thayer, J. G., Thomas, S., Thornton, A. J., Thukral, V., Tice, J., Trilling, D. E., Turri, M., Van Berg, R., Vanden Berk, D., Vetter, K., Virieux, F., Vucina, T., Wahl, W., Walkowicz, L., Walsh, B., Walter, C. W., Wang, D. L., Wang, S.-Y., Warner, M., Wiecha, O., Willman, B., Winters, S. E., Wittman, D., Wolff, S. C., Wood-Vasey, W. M., Wu, X., Xin, B., Yoachim, P. and Zhan, H. (2019) LSST: From science drivers to reference design and anticipated data products. *Astrophys. J.*, 873(2), 111. <https://doi.org/10.3847/1538-4357/ab042c>.

Keller, P. M., Breedt, E., Hodgkin, S., Belokurov, V., Wild, J., García-Soriano, I. and Wise, J. L. (2022) Eclipsing white dwarf binaries in *Gaia* and the Zwicky Transient Facility. *Mon. Not. R. Astron. Soc.*, 509(3), 4171–4188. <https://doi.org/10.1093/mnras/stab3293>.

Kepler, S. O., Pelisoli, I., Koester, D., Ourique, G., Kleinman, S. J., Romero, A. D., Nitta, A., Eisenstein, D. J., Costa, J. E. S., Külebi, B., Jordan, S., Dufour, P., Giommi, P. and Rebassa-Mansergas, A. (2015) New white dwarf stars in the Sloan Digital Sky Survey Data Release 10. *Mon. Not. R. Astron. Soc.*, 446(4), 4078–4087. <https://doi.org/10.1093/mnras/stu2388>.

Koen, C., O'Donoghue, D., Pollacco, D. L. and Nitta, A. (1998) The EC 14026 stars – XI. Feige 48: a link in its class. *Mon. Not. R. Astron. Soc.*, 300(4), 1105–1110. <https://doi.org/10.1046/j.1365-8711.1998.01983.x>.

Kupfer, T., Bauer, E. B., Burdge, K. B., Roestel, J. v., Bellm, E. C., Fuller, J., Hermes, J., Marsh, T. R., Bildsten, L., Kulkarni, S. R., Phinney, E. S., Prince, T. A., Szkody, P., Yao, Y., Irrgang, A., Heber, U., Schneider, D., Dhillon, V. S., Murawski, G., Drake, A. J., Duev, D. A., Feeney, M., Graham, M. J., Laher, R. R., Littlefair, S. P., Mahabal, A. A., Masci, F. J., Porter, M., Reiley, D., Rodriguez, H., Rusholme, B., Shupe, D. L. and Soumagnac, M. T. (2020) A new class of Roche lobe–filling hot subdwarf binaries. *Astrophys. J. Lett.*, 898(1), L25. <https://doi.org/10.3847/2041-8213/aba3c2>.

Latour, M., Fontaine, G. and Green, E. (2014a) Updates on the pulsating sdB star Feige 48 through spectroscopy. In 6th Meeting on Hot Subdwarf Stars and Related Objects, edited by van Grootel, V., Green, E., Fontaine, G. and Charpinet, S., vol. 481 of *Astronomical Society of the Pacific Conference Series*, p. 91.

Latour, M., Fontaine, G., Green, E. M., Brassard, P. and Chayer, P. (2014b) Improved determination of the atmospheric parameters of the pulsating sdB star Feige 48. *Astrophys. J.*, 788(1), 65. <https://doi.org/10.1088/0004-637X/788/1/65>.

Lei, Z., Zhao, J., Németh, P. and Zhao, G. (2019) New hot subdwarf stars identified in *Gaia* DR2 with LAMOST DR5 spectra. II. *Astrophys. J.*, 881(2), 135. <https://doi.org/10.3847/1538-4357/ab2edc>.

LSST Science Collaboration, Abell, P. A., Allison, J., Anderson, S. F., Andrew, J. R., Angel, J. R. P., Armus, L., Arnett, D., Asztalos, S. J., Axelrod, T. S., Bailey, S., Ballantyne, D. R., Bankert, J. R., Barkhouse, W. A., Barr, J. D., Barrientos, L. F., Barth, A. J., Bartlett, J. G., Becker, A. C., Becla, J., Beers, T. C., Bernstein, J. P., Biswas, R., Blanton, M. R., Bloom, J. S., Bochanski, J. J., Boeshaar, P., Borne, K. D., Bradac, M., Brandt, W. N., Bridge, C. R., Brown, M. E., Brunner, R. J., Bullock, J. S., Burgasser, A. J., Burge, J. H., Burke, D. L., Cargile, P. A., Chandrasekharan, S., Chartas, G., Chesley, S. R., Chu, Y.-H., Cinabro, D., Claire, M. W., Claver, C. F., Clowe, D., Connolly, A. J., Cook, K. H., Cooke, J., Cooray, A., Covey, K. R., Culliton, C. S., de Jong, R., de Vries, W. H., Debattista, V. P., Delgado, F., Dell'Antonio, I. P., Dhital, S., Di Stefano, R., Dickinson, M., Dilday, B., Djorgovski, S. G., Dobler, G., Donalek, C., Dubois-Felsmann, G., Durech, J., Eliasdottir, A., Eracleous, M., Eyer, L., Falco, E. E., Fan, X., Fassnacht, C. D., Ferguson, H. C., Fernandez, Y. R., Fields, B. D., Finkbeiner, D., Figueroa, E. E., Fox, D. B., Francke, H., Frank, J. S., Frieman, J., Fromenteau, S., Furqan, M., Galaz, G., Gal-Yam, A., Garnavich, P., Gawiser, E., Geary, J., Gee, P., Gibson, R. R., Gilmore, K., Grace, E. A., Green, R. F., Gressler, W. J., Grillmair, C. J., Habib, S., Haggerty, J. S., Hamuy, M., Harris, A. W., Hawley, S. L., Heavens, A. F., Hebb, L., Henry, T. J., Hileman, E., Hilton, E. J., Hoadley, K., Holberg, J. B., Holman, M. J., Howell, S. B., Infante, L., Ivezić, Z., Jacoby, S. H., Jain, B., R., Jedicke, Jee, M. J., Garrett Jernigan, J., Jha, S. W., Johnston, K. V., Jones, R. L., Juric, M., Kaasalainen, M., Stylianis, Kafka, Kahn, S. M., Kaib, N. A., Kalirai, J., Kantor, J., Kasliwal, M. M., Keeton, C. R., Kessler, R., Knezevic, Z., Kowalski, A., Krabbendam, V. L., Krughoff, K. S., Kulkarni, S., Kuhlman, S., Lacy, M., Lepine, S., Liang, M., Lien, A., Lira, P., Long, K. S., Lorenz, S., Lotz, J. M., Lupton, R. H., Lutz, J., Macri, L. M., Mahabal, A. A., Mandelbaum, R., Marshall, P., May, M., McGehee, P. M., Meadows, B. T., Meert, A., Milani, A., Miller, C. J., Miller, M., Mills, D., Minniti, D., Monet, D., Mukadam, A. S., Nakar, E., Neill, D. R., Newman, J. A., Nikolaev, S., Nordby, M., O'Connor, P., Oguri, M., Oliver, J., Olivier, S. S., Olsen, J. K., Olsen, K., Olszewski, E. W., Oluseyi, H., Padilla, N. D., Parker, A., Pepper, J., Peterson, J. R., Petry, C., Pinto, P. A., Pizagno, J. L., Popescu, B., Prsa, A., Radcka, V., Raddick, M. J., Rasmussen, A., Rau, A., Rho, J., Rhoads, J. E., Richards, G. T., Ridgway, S. T., Robertson, B. E., Roskar, R., Saha, A., Sarajedini, A., Scannapieco, E., Schalk, T., Schindler, R., Schmidt, S., Schmidt, S., Schneider, D. P., Schumacher, G., Scranton, R., Sebag, J., Seppala, L. G., Shemmer, O., Simon, J. D., Sivertz, M., Smith, H. A., Allyn Smith, J., Smith, N., Spitz, A. H., Stanford, A., Stassun, K. G., Strader, J., Strauss, M. A., Stubbs, C. W., Sweeney, D. W., Szalay, A., Szkody, P., Takada, M., Thorman, P., Trilling, D. E., Trimble, V., Tyson, A., Van Berg, R., Vanden Berk, D., VanderPlas, J., Verde, L., Vršnak, B., Walkowicz, L. M., Wandelt, B. D., Wang, S., Wang, Y., Warner, M., Wechsler, R. H., West, A. A., Wiecha, O., Williams, B. F., Willman, B., Wittman, D., Wolff, S. C., Wood-Vasey, W. M., Wozniak, P., Young, P., Zentner, A. and Zhan, H. (2009) LSST Science Book, Version 2.0. arXiv e-prints, arXiv:0912.0201.

Masci, F. J., Laher, R. R., Rusholme, B., Shupe, D. L., Groom, S., Surace, J., Jackson, E., Monkewitz, S., Beck, R., Flynn, D., Terek, S., Landry, W., Hacopians, E., Desai, V., Howell, J., Brooke, T., Imel, D., Wachter, S., Ye, Q.-Z., Lin, H.-W., Cenko, S. B., Cunningham,

V., RebbaPragada, U., Bue, B., Miller, A. A., Mahabal, A., Bellm, E. C., Patterson, M. T., Jurić, M., Golkhou, V. Z., Ofek, E. O., Walters, R., Graham, M., Kasliwal, M. M., Dekany, R. G., Kupfer, T., Burdge, K., Cannella, C. B., Barlow, T., Van Sistine, A., Giomi, M., Fremling, C., Blagorodnova, N., Levitan, D., Riddle, R., Smith, R. M., Helou, G., Prince, T. A. and Kulkarni, S. R. (2019) The Zwicky Transient Facility: Data processing, products, and archive. *Publ. Astron. Soc. Pac.*, 131(995), 018003. <https://doi.org/10.1088/1538-3873/aae8ac>.

Menzies, J. W. and Marang, F. (1986) A new B-subdwarf eclipsing binary with an extremely short period. In *Instrumentation and Research Programmes for Small Telescopes*, edited by Hearnshaw, J. B. and Cottrell, P. L., vol. 118, p. 305.

Paczynski, B. (1976) Common envelope binaries. In *Structure and Evolution of Close Binary Systems*, edited by Eggleton, P., Mitton, S. and Whelan, J., vol. 73, p. 75.

Pietrukowicz, P., Mróz, P., Soszyński, I., Udalski, A., Poleski, R., Szymański, M. K., Kubiak, M., Pietrzyński, G., Wyrzykowski, Ł., Ulaczyk, K., Kozłowski, S. and Skowron, J. (2013) Eclipsing binary stars in the OGLE-III Galactic disk fields. *Acta Astron.*, 63(2), 115–133. https://acta.astrouw.edu.pl/Vol63/n2/pdf/pap_63_2_1.pdf.

Saffer, R. A., Bergeron, P., Koester, D. and Liebert, J. (1994) Atmospheric parameters of field subdwarf B stars. *Astrophys. J.*, 432, 351. <https://doi.org/10.1086/174573>.

Schaffenroth, V., Barlow, B. N., Geier, S., Vučković, M., Kilkenny, D., Wolz, M., Kupfer, T., Heber, U., Drechsel, H., Kimeswenger, S., Marsh, T., Wolf, M., Pelisoli, I., Freudenthal, J., Dreizler, S., Kreuzer, S. and Ziegerer, E. (2019) The EREBOS project: Investigating the effect of substellar and low-mass stellar companions on late stellar evolution. Survey, target selection, and atmospheric parameters. *Astron. Astrophys.*, 630, A80. <https://doi.org/10.1051/0004-6361/201936019>.

Schaffenroth, V., Geier, S., Barbu-Barna, I., Heber, U., Kupfer, T. and Cordes, O. (2014) New HW Virginis systems from the MUCHFUSS project. In *6th Meeting on Hot Subdwarf Stars and Related Objects*, edited by van Grootel, V., Green, E., Fontaine, G. and Charpinet, S., vol. 481 of *Astronomical Society of the Pacific Conference Series*, p. 253.

Schaffenroth, V., Pelisoli, I., Barlow, B. N., Geier, S. and Kupfer, T. (2022) Hot subdwarfs in close binaries observed from space I: orbital, atmospheric, and absolute parameters and the nature of their companions. *arXiv e-prints*, arXiv:2207.02001.

Soszyński, I., Pawlak, M., Pietrukowicz, P., Udalski, A., Szymański, M. K., Wyrzykowski, Ł., Ulaczyk, K., Poleski, R., Kozłowski, S., Skowron, D. M., Skowron, J., Mróz, P. and Hamanowicz, A. (2016) The OGLE collection of variable stars. Over 450 000 eclipsing and ellipsoidal binary systems toward the Galactic bulge. *Acta Astron.*, 66(4), 405–420. https://acta.astrouw.edu.pl/Vol66/n4/pdf/pap_66_4_1.pdf.

Tody, D. (1986) The IRAF data reduction and analysis system. In Proc. SPIE, edited by Crawford, D. L., vol. 627 of *Society of Photo-Optical Instrumentation Engineers (SPIE) Conference Series*, p. 733. <https://doi.org/10.1117/12.968154>.

Tonry, J. L., Denneau, L., Heinze, A. N., Stalder, B., Smith, K. W., Smartt, S. J., Stubbs, C. W., Weiland, H. J. and Rest, A. (2018) ATLAS: A high-cadence all-sky survey system. *Publ. Astron. Soc. Pac.*, 130(988), 064505. <https://doi.org/10.1088/1538-3873/aabadf>.

VanderPlas, J. T. and Ivezić, Ž. (2015) Periodograms for multiband astronomical time series. *Astrophys. J.*, 812(1), 18. <https://doi.org/10.1088/0004-637X/812/1/18>.